ENVIRONMENTAL RESEARCH
CLIMATE

PURPOSE-LED PUBLISHING™ Part of the ENVIRONMENTAL RESEARCH SERIES

PAPER • OPEN ACCESS

Assessing the impact of stratospheric aerosol injection on precipitation extremes in Africa using the ARISE-SAI-1.5 dataset

To cite this article: Kwesi A Quagraine *et al* 2025 *Environ. Res.: Climate* **4** 035006

ENVIRONMENTAL RESEARCH
CLIMATE

PAPER

Assessing the impact of stratospheric aerosol injection on precipitation extremes in Africa using the ARISE-SAI-1.5 dataset

Kwesi A Quagraine[1,2,3,*], **Mari R Tye**[1,4], **Kwesi T Quagraine**[5], **Simone Tilmes**[1], **Isla R Simpson**[1], **Francis Nkrumah**[3], **Temitope S Egbebiyi**[2], **Romaric C Odoulami**[6] **and Nana Ama Browne Klutse**[7]

[1] NSF National Center for Atmospheric Research, Boulder, CO, United States of America
[2] Climate System Analysis Group, University of Cape Town, Cape Town, South Africa
[3] Department of Physics, University of Cape Coast, Cape Coast, Ghana
[4] Whiting School of Engineering, Johns Hopkins University, Baltimore, MD, United States of America
[5] Department of Earth and Atmospheric Science, Indiana University, Bloomington, IN, United States of America
[6] African Climate and Development Initiative, University of Cape Town, Cape Town, South Africa
[7] Department of Physics, University of Ghana, Accra, Ghana
[*] Author to whom any correspondence should be addressed.

E-mail: kwsquagraine@gmail.com

Keywords: solar radiation modifications Africa, SAI precipitation, extreme precipitation under SAI Africa, ARISE-SAI-1.5, stratospheric aerosol injection impacts - Africa, precipitation extremes - Africa

Supplementary material for this article is available online

OPEN ACCESS

RECEIVED
15 February 2025

REVISED
26 June 2025

ACCEPTED FOR PUBLICATION
10 July 2025

PUBLISHED
22 July 2025

Abstract

Stratospheric aerosol injection (SAI) is a proposed climate intervention method aimed at mitigating some of the impacts of anthropogenic global warming by enhancing the atmosphere's reflectivity, thus reducing solar radiation reaching the Earth's surface. While SAI's extreme temperature-reducing effects are well-established, its impact on precipitation extremes remains uncertain, especially in Africa, a region highly vulnerable to climate change. Understanding SAI's potential effects on precipitation extremes is crucial, as it could increase or decrease variability in precipitation patterns, thereby affecting food security and ecosystems. Our findings indicate that areas projected under SSP2-4.5 to experience intense precipitation, such as parts of West and Central Africa, are projected to experience a reduction in both the frequency and intensity of precipitation, whereas drier areas are expected to receive increased precipitation under the SSP2-4.5 scenario with SAI. Also, the response to this SAI scenario varies considerably across different regions, displaying a high degree of heterogeneity across multiple precipitation extreme indices. These findings underscore the need to explore other scenarios of SAI and for further regional studies to understand SAI's implications better and to inform climate-policy decisions.

1. Introduction

Stratospheric aerosol injection (SAI), a form of solar geoengineering, has emerged as a potential strategy to mitigate some effects of global warming by reflecting a portion of incoming solar radiation back into space (Crutzen 2006, Robock *et al* 2009). By injecting aerosols, such as sulfate particles or their precursors, into the stratosphere, SAI aims to reduce surface temperatures and, in effect, general circulation patterns that induce more projected extremes under the Shared Socio-economic Pathway, SSP2-4.5 (Robock *et al* 2008, Tilmes *et al* 2018). However, the implementation of SAI remains highly contentious, with major uncertainties persisting regarding its regional climate impacts, particularly on precipitation patterns and extremes (Burns *et al* 2016, Carlson and Trisos 2018, Irvine *et al* 2020, Usha *et al* 2024).

Africa is particularly vulnerable to changes in precipitation due to its reliance on rain-fed agriculture, hydropower, variable climate, and socio-economic challenges (Serdeczny *et al* 2017). The continent experiences both prolonged droughts and intense rainfall extremes, each of which is expected to worsen under climate change (Niang *et al* 2014, Sylla *et al* 2016, Klutse *et al* 2018, Donat *et al* 2020, Haile *et al* 2020, IPCC 2021, Blunden *et al* 2024). The erratic onset, cessation, and duration of the rainy season (Akinsanola

et al 2020, Kumi *et al* 2018) cause serious repercussions on health, agriculture, and the economy, leading to crop failures and loss of life (Di Baldassarre *et al* 2010, Vogel *et al* 2019, Simanjuntak *et al* 2023). Consequently, food security, water resources, and overall regional stability are at significant risk. Understanding how SAI might alter these precipitation extremes in the presence of continued greenhouse gas-driven warming is crucial for a region whose climate is closely tied to agricultural productivity and water resources. Assessing the combined effects of SAI and elevated greenhouse gases relative to a warming scenario without SAI can provide critical insight into the potential shifts in extreme weather that could severely impact food and water security, disrupt ecosystems, and affect livelihoods.

While SAI's cooling effects are well-documented, its impact on precipitation patterns remains uncertain (Ji *et al* 2018, Irvine and Keith 2020, Liu *et al* 2022). This paper examines the potential near-and mid-century changes in Africa's precipitation extremes under the SSP2-4.5 scenario with SAI deployment while quantifying the relative differences between SSP2-4.5 and SAI scenarios compared to the control period. Specifically, it investigates whether SAI can mitigate changes in the intensity and frequency of precipitation extremes across Africa, assuming global mean temperature is controlled to 1.5 °C above pre-industrial levels, compared to ongoing anthropogenic greenhouse gas emissions alone. This scenario aligns with the target of the Paris Agreement and represents a climate future that prioritizes some mitigation efforts.

Recent studies (e.g. Pinto *et al* 2020, Tye *et al* 2022) have analyzed the impact of SAI on precipitation extremes over Africa and globally under the high-emission representative concentration pathway (RCP) 8.5 scenario. Their findings indicate that extreme precipitation generally decreases in currently wet regions and increases in drier areas, following a 'wet-gets-drier, dry-gets-wetter' pattern. Additionally, under RCP8.5, SAI reduces the intensity of extreme precipitation events, increases the frequency of light rain days, and shortens the duration of long wet and dry spells.

Our study uses a geoengineering dataset based on the SSP2-4.5 scenario instead of RCP8.5 to provide a more policy-relevant assessment of climate extremes under SAI. SSP2-4.5 represents a moderate emissions pathway, reflecting current global climate policies and socioeconomic trends, making it a more realistic baseline for future climate projections. In contrast, RCP8.5, originally designed as a high-end, worst-case scenario, assumes unrestricted fossil fuel use and extreme warming, which is now considered unlikely given ongoing mitigation efforts and the global transition to renewable energy. By using SSP2-4.5, our analysis better aligns with contemporary climate governance, providing insights that are more applicable to policy decisions and risk assessments. This approach allows us to explore plausible trade-offs and benefits of climate intervention strategies while avoiding the overestimation of risks associated with unrealistic emissions trajectories. However, we acknowledge key differences between our results and studies using RCP8.5. The following sections detail the data and methods used, discuss the results, and present our conclusions.

2. Data and methods

2.1. Data

This study uses the output from the 'Assessing responses and impacts of solar climate intervention on the earth with SAI' (ARISE-SAI-1.5, hereafter SAI1.5) experiment (Richter *et al* 2022), which was carried out with the NSF NCAR's community earth system model version 2 (CESM2; Danabasoglu *et al* 2020) and the high-top atmospheric model component, whole atmosphere community climate model version 6 (WACCM6; Gettelman *et al* 2019), to investigate the impacts of SAI. WACCM6 (hereafter WACCM) can accurately capture the microphysical and chemical processes associated with stratospheric aerosols, as well as their interactions with the climate system in the context of large volcanic eruptions, which are somewhat analogous to SAI (Mills *et al* 2017). We use four historical members of WACCM that were then branched into four SSP2-4.5 members in 2015.

The SAI1.5 experiment consists of 10 members, with the first five members (members 001–005) based on the corresponding SSP2-4.5 simulations done with CESM2 (WACCM6) and starting in 2035, of those SSP2-4.5 simulations when the aerosol injections began. Each of these members had different starting points for the ocean, sea ice, land, and atmosphere as of 1 January 2035, i.e. the 'macro' method of initialization (Hawkins *et al* 2016). Just like the SSP2-4.5 simulations, the next set of members (006–010) was initialized using the same starting points as the first five but with a small temperature perturbation added to the atmosphere to create some variation among the ensemble members i.e. the 'micro' method of initialization (Hawkins *et al* 2016).

It is, however, important to acknowledge potential biases related to the model's resolution and the representation of sub-grid scale processes through parameterization and the inherent limitations in capturing localized extreme events. The reader is referred to Richter *et al* (2022) for a detailed description of the SAI1.5 experimental setup and MacMartin *et al* (2022) for the rationale behind the scenarios chosen. Using SSP2-4.5 (O'Neill *et al* 2016) as a baseline scenario, a simulation covering the years 2015–2069 was

Table 1. Expert team on climate change detection and indices (ETCCDI) based definitions of selected extreme indices (Zhang *et al* 2011; https://etccdi.pacificclimate.org/list_27_indices.shtml).

Index	Descriptive name	Definition	Units
PRCPTOT	Total rainfall	Annual sum of precipitation (PR)	mm yr^{-1}
RX1D	Wettest day	Annual maximum 1 d precipitation	mm d^{-1}
RX5D	Wettest pentad	Annual maximum consecutive 5 d precipitation	mm 5 d^{-1}
SDII	Simple daily intensity	The ratio of annual total precipitation to the number of wet days ($\geqslant$1 mm)	mm d^{-1}
R20mm	Very heavy precipitation days	Number of days per year when precipitation $\geqslant$20 mm	days yr^{-1}
CDD	Consecutive dry days	Maximum number of consecutive days per year when precipitation $<$1 mm	days yr^{-1}
CWD	Consecutive wet days	Maximum number of consecutive days per year when precipitation $\geqslant$1 mm	days yr^{-1}
N95	Frequency of very wet days	Number of days per year when precipitation exceeds the 2015–2030 mean 95th percentile	days yr^{-1}
R95p	Very wet days of precipitation	Annual total precipitation from daily precipitation $>$95th percentile	mm yr^{-1}

conducted. This SSP2-4.5 scenario is relatively close to the emissions trajectory of recent years and close to projected emission trajectories (Hausfather and Peters 2020a).

The results section compares the SSP2-4.5 simulation with the SAI1.5 perturbation experiment. To achieve this, sulfur dioxide is strategically injected at four latitudinal positions (15° S, 15° N, 30° S, 30° N) within a single grid box situated at 180°longitude enclosed by two pressure interfaces (47.1 hPa and 39.3 hPa), which is approximately comparable to a geometric altitude of 21.6 km at the midpoint of the grid box. This choice of injection sites allows for autonomous management of the desired climate targets using feedback control systems. The key climate targets include limiting the global mean surface temperature (GMST) near 1.5 K above pre-industrial levels and maintaining the inter-hemispheric temperature gradient balance (Kravitz *et al* 2017, Richter *et al* 2022). While the technology does not currently exist to reach an injection altitude of 21.6 km, it is possible to use existing aircraft technologies, which could be modified to operate as climate intervention aircraft (Bingaman *et al* 2020).

The model's ability to capture the rainfall patterns over the region is assessed by comparing model outputs with observed data from the Climate Hazards Group Infrared Precipitation with Stations (CHIRPS) dataset from 1981 to 2025 at 0.05° (∼5 km) spatial resolution (Funk *et al* 2015). CHIRPS is particularly valuable for regions like Africa with sparse observational coverage and accurately captures precipitation variability across the continent (Quagraine *et al* 2020, Gbode *et al* 2023). This comparison is crucial for assessing the model's ability to reproduce the present-day climate, a key step in building confidence in its future projections.

2.2. Methods

WACCM's ability to simulate precipitation over Africa is evaluated against the CHIRPS dataset over a common period of 1981–2015. As part of this evaluation, we evaluated WACCM within the context of the uncertainty due to internal variability by identifying grid points where the observed precipitation lies outside the spread of the climatologies of the four WACCM historical ensemble members. Additionally, the seasonal cycles of WACCM and CHIRPS were compared, and uncertainties on the WACCM climatology were quantified by calculating the standard error on the ensemble mean as $\sigma/\sqrt{4}$ where σ is the standard deviation across the four ensemble members.

We assessed projected changes in precipitation extremes over Africa with SAI1.5 and the SSP2-4.5 scenarios using 9 climate indices (table 1) based on the definitions of the World Meteorological Organization Expert team on climate change detection and indices (ETCCDI; Zhang *et al* 2011). The climate indices have been calculated on an annual scale.

As our present-day climate (hereafter control period; CTL), we used the moderate emission scenario, SSP2-4.5 from 2015–2035. Future changes are assessed under the moderate emission scenario (SSP2-4.5) by comparing the mean future period (2035–2069) for that scenario with the CTL period. The future is divided into near-future (2035–2054), marking the SAI1.5 deployment phase, and mid-future (2050–2069), representing the stabilization of SO_2 injection rates as per MacMartin *et al* (2019). The year 2035 marks the start of SAI1.5 intervention and the decade when simulations crossed the GMST of 1.5 K, while 2050 is

crucial for evaluating long-term impacts post-stabilization. The intentional overlap between these two periods reflects the gradual transition from deployment ramp-up to stabilization, enabling a more continuous assessment of SAI's evolving climate impacts. This study aims to capture key changes under SSP2-4.5 with and without SAI1.5, focusing on these two periods to evaluate the potential of SAI1.5 to mitigate or exacerbate the projected impacts of SSP2-4.5 on future climate extremes. The significance of the difference between SAI1.5 and SSP2-4.5 is determined using a one-sided Student's *t*-test (Snedecor 1989) on the difference between the two ensemble member sets of 20 year climatologies, treating each member's 20 year climatology as an independent sample. Lydersen (2014) explains the advantages of a Student's *t*-test for such applications.

To quantify changes in precipitation extremes, we use barplots and violin plots, which incorporate Kernel density estimation (KDE). KDE provides qualitative and quantitative distribution, skewness, and probability density of the data, including the likelihood of extreme events. These extremes are inferred from the tails of the distribution; longer and thinner tails indicate a higher probability of extreme events (i.e. values approximately two standard deviations beyond the mean).

We reiterate that these results provide an assessment of projected changes in extreme precipitation over Africa under the SAI1.5 scenario and should be interpreted with caution, as this represents just one perspective of the potential response to SAI in general.

3. Results

3.1. Evaluation of model performance in simulating rainfall

To build confidence in WACCM's ability to accurately project future climate change, we first evaluated its ability to capture precipitation patterns over Africa for the present day. The analysis is summarized across five sub-regions: North Africa (NAF), West Africa (WAF), East Africa (EAF), Central Africa (CAF), and Southern Africa (SAF).

In figure 1, we examine the spatial climatology, model bias, and the 95th percentile bias of daily precipitation for each year averaged across all the years over Africa (a)–(c) and the seasonal cycle over the five sub-regions (d)–(h). The stippling on figure 1(b) indicates areas where CHIRPS observations lie outside the distribution of the ensemble members from WACCM, signifying regions where the model bias is statistically significant. Notably, positive precipitation bias (up to 60 mm month^{-1}) is typically concentrated over the equatorial regions; WAF, CAF, and EAF, and the southern parts of the continent; SAF, while NAF shows drier conditions (up to 10 mm month^{-1}). A high degree of agreement between WACCM and CHIRPS observations (pattern correlation of 0.96) suggests that, despite localized biases, the model qualitatively captures the spatial variations in precipitation.

We examine the bias of the 95th percentile of wet-day precipitation in the model for an indication of how it accurately captures extreme precipitation as compared to the CHIRPS observations. The model significantly overestimates the magnitude of extreme precipitation events in the relatively dry NAF and SAF regions. Also, there is moderate to weak overprediction in other regions compared to NAF and SAF. This has been attributed in part to the influence of complex topography on precipitation patterns and is not exclusive to WACCM but to most models in general (e.g. Nikulin *et al* 2012, Sylla *et al* 2013).

WACCM reasonably captures the seasonal progression of precipitation across Africa as represented by CHIRPS, particularly the timing of the wet and dry seasons (figures 1(d)–(h)). However, systematic biases are evident. The model overestimates precipitation in certain months across NAF (e.g. April–June) and SAF (e.g. February to September), while it underestimates rainfall over WAF (e.g. July–September), EAF (e.g. March–November), and CAF throughout most of the year (figures 1(d)–(h)). These biases are reflected in root mean square error values from ∼3 mm d^{-1} in NAF to 21 mm d^{-1} in CAF (table S1). Despite these discrepancies in magnitude, WACCM captures the broad seasonal structure of rainfall well enough to support the analyses we pursue.

3.2. Implications of SAI1.5 for extreme precipitation indices

3.2.1. Annual totals and heavy rainfall extremes

Figure 2 presents changes in total annual precipitation (PRCPTOT), extreme daily (RX1D), 5 day (RX5D) rainfall, very wet day totals (R95p), and the frequency of very wet days (N95).

Under SSP2-4.5, PRCPTOT is projected to increase substantially in EAF and CAF by +60 to +120 mm yr^{-1}, while decreases of −20 to −140 mm yr^{-1} dominate WAF and NAF (figure 2(a)). For SAI1.5 over the control period (figure 2(b)), the signal is reversed across many regions, especially over CAF, southern WAF, and SAF, where projected reductions reach −40 to −90 mm yr^{-1}. The intervention of SAI1.5 significantly impacts the projected change in the mid-future by significantly reducing PRCPTOT over the EAF, CAF, and northern SAF (figure 2(c)) and increasing PRCPTOT over western WAF A similar spatial

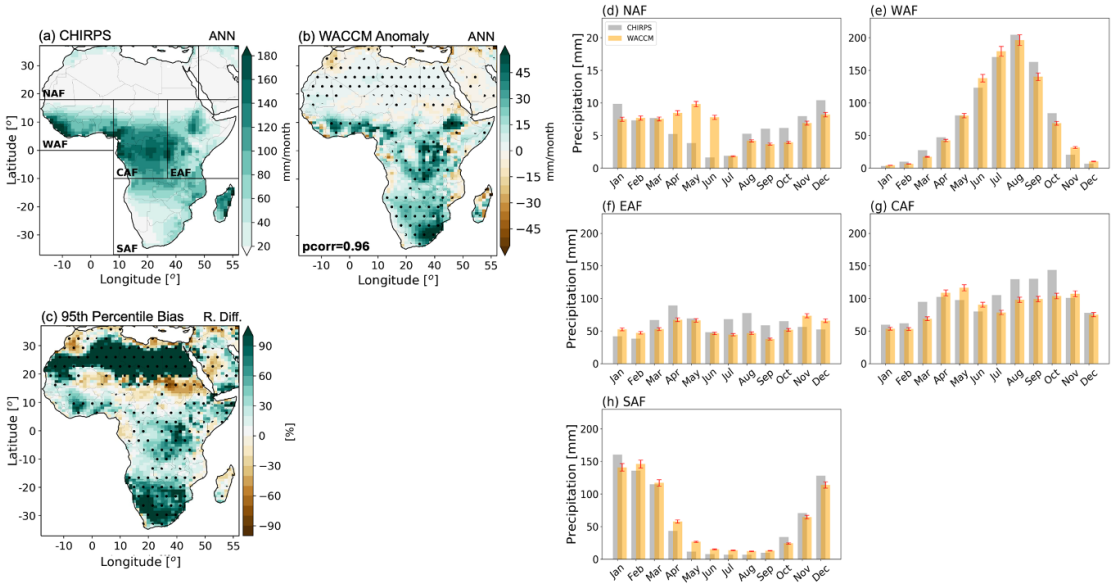

Figure 1. Annual (ANN) climatology of precipitation for the period 1981–2015 from CHIRPS (a), model bias during 1981–2015 relative to CHIRPS climatology with stippling indicating grid points where observation lies outside the distribution of the ensemble members of the model (b), and 95th percentile bias expressed as relative difference (R. Diff.) from CHIRPS with stippling indicating grid points where changes are significant at 5% level using the one-sided Student's *t*-test (c). Pattern correlation between WACCM and CHIRPS is shown in the bottom left of (b). The seasonal cycle of Precipitation (d)–(h) for each African region is denoted by: WAF—West Africa, EAF—East Africa, NAF—North Africa, CAF—Central Africa, and SAF—Southern Africa, as shown in (a). Note the different *y*-axis range on panel (d) compared to the others.

pattern of the impact of SAI1.5 is noted for the near-future period, albeit with lower intensities of PRCPTOT, change across all regions (figures S1(a)–(c)). These projected decreases in PRCPTOT have been attributed to a shift towards days with less intense rain and fewer very intense rain days (Camilloni *et al* 2022, Tye *et al* 2022).

For RX1D and RX5D (figures 2(d)–(i)), which represent daily and 5 d heavy precipitation extremes, SSP2-4.5 induces increases of +6 mm d^{-1} to +15 mm 5 d^{-1} respectively in EAF and SAF respectively. In contrast, SAI1.5 substantially weakens these extremes, especially over SAF and central regions, leading to reductions of ∼5 mm d^{-1}–30 mm 5 d^{-1} in both RX1D and RX5D (figures 2(f) and (i)). For the near-future period, areas show similar responses for both RX1D (figures S1(d)–(f)) and RX5D (figures S1(g)–(i)), although their magnitudes are much smaller in comparison with the mid-future period.

The R95p, the total precipitation from very wet days of precipitation index (figures 2(j)–(l)), reveals the largest SSP2-4.5-driven increases (+80 mm yr^{-1}) in EAF and CAF, alongside decreases in western WAF (–25 mm yr^{-1}). These increases are mitigated under SAI1.5, with large reductions across southern WAF (–30 mm yr^{-1}), CAF and EAF (–00 mm yr^{-1}) (figure 2(l)).

The N95 index, representing the number of very wet days per year (figures 2(m)–(o)), increases under SSP2-4.5 by 1 to days yr^{-1} in EAF and CAF, while under SAI1.5 with respect to control period, these increases are either diminished or reversed across SAF and WAF (−0.5 to −1.5 d yr^{-1}). Under SAI1.5 (figure 2(o)) there are significant reductions in very wet days compared to SSP2-4.5. The response is consistent across sub-regions in the near future (figures S1(j)–(l)). We also note that increases and decreases in the N95 index generally coincide with areas of significant changes in the R95p index.

3.2.2. Dry spells, persistent rainfall, and rainfall intensity

The projected changes in dry and wet spell behavior, along with rainfall frequency and intensity, are shown in figure 3. Consecutive dry days (CDD) under SSP2-4.5 (figure 3(a)) are projected to increase markedly over western NAF and southeastern SAF (+6 to +12 d yr^{-1}), while reductions occur in EAF and central to eastern NAF (−6 to −18 d yr^{-1}). SAI1.5 relative to control period (figure 3(b)) shows an amplification of CDD across SAF and CAF (∼14 d yr^{-1}) and reduces dry spell durations in NAF and WAF. The response under SSP2-4.5 is largely offset in parts of WAF although an increase is western CAF persists (figure 3(c)).

In contrast, consecutive wet days (CWD) is projected to decrease under SSP2-4.5 by −4 to −16 d yr^{-1} along the Gulf of Guinea and CAF (figure 3(d)). Under SAI1.5 relative to the control period (figure 3(e)), CWD is projected to decrease in the magnitude of this pattern, yielding −2 to −4 d yr^{-1}, particularly over

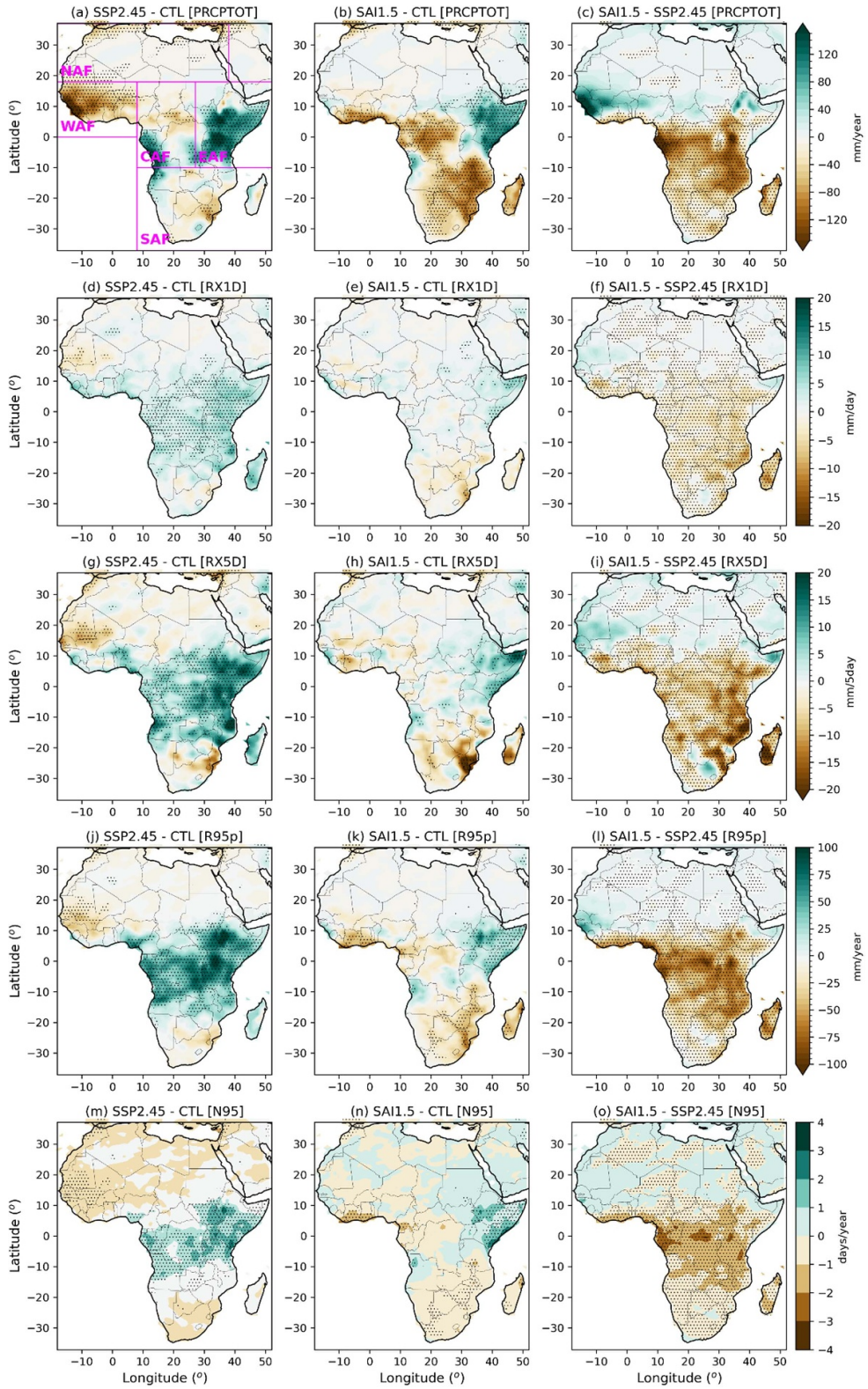

Figure 2. Projected changes in total rainfall, wettest day, wettest pentad, very wet days precipitation, and very wet days (PRCPTOT, RX1D, RX5D, R95p, N95) for the mid-future period (2050–2069) relative to the control period (CTL; 2015–2034). Panels (a), (d), (g), (j) and (m) show changes under SSP2-4.5, panels (b), (e), (h), (k) and (n) under SAI1.5, and panels (c), (f), (i), (l) and (o) show the difference between SAI1.5 and SSP2-4.5. The five African sub-regions used in the analysis are shown in (a). Stippling indicates grid points where changes are significant at the 5% level using the one-sided Student's *t*-test.

CAF and southern WAF. SAI1.5 flips the drying in these regions with increased wet days (+3 to +6 d yr^{-1}) (figure 3(f)).

For R20mm (figures 3(g)–(i)), SSP2-4.5 projects slight increases in EAF and CAF (+1 to +6 d yr^{-1}), with decreases of −1 to −6 d yr^{-1} across western WAF. SAI1.5, relative to control period, moderates these

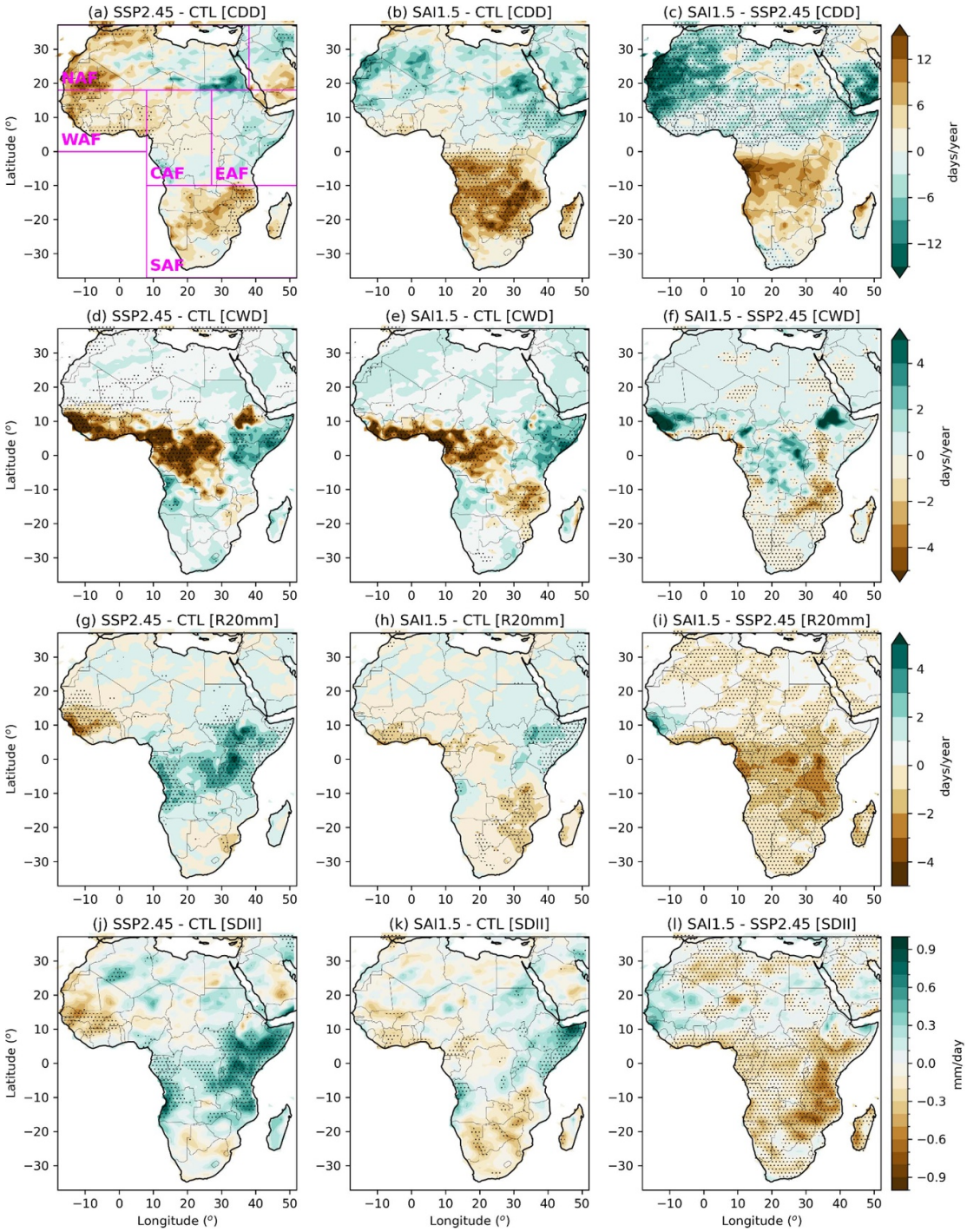

Figure 3. Projected changes in consecutive dry days (CDD), consecutive wet days (CWD), very heavy precipitation days (R20 mm), and the simple daily intensity index (SDII) for the mid-future period (2050–2069) relative to the control period (CTL; 2015–2034). Panels (a), (d), (g) and (j) show changes under SSP2-4.5, panels (b), (e), (h) and (k) under SAI1.5, and panels (c), (f), (i) and (l) show the difference between SAI1.5 and SSP2-4.5. The five African sub-regions used in the analysis are shown in (a). Stippling indicates grid points where changes are significant at 5% level using the one-sided Student's t-test.

shifts (figure 3(h)), resulting in mostly neutral responses (-2 to $+2$ d yr^{-1}). The responses in the SSP2-4.5 are offset under SAI1.5 with CAF and EAF projected to experience widespread reductions (-2 to -6 d yr^{-1}) in very heavy rainfall days (figure 3(i)).

The simple daily intensity index (SDII), which reflects average rainfall intensity on wet days, increases by $+0.3$ to $+1$ mm d^{-1} in EAF and CAF under SSP2-4.5 (figure 3(j)), while SAI1.5 with respect to control shows moderate responses across most regions to -0.3 to $+0.6$ mm dayr^{-1} (figure 3(k)). SAI1.5 largely mitigates the impacts of climate change, reducing the increase in SDII produced by SSP2-4.5 (figure 3(l)) leaving relatively muted changes (figure 3(k)). A similar pattern is observed in the near-future period with lower magnitudes (figures S2(j)–(l)). These changes are consistent with the near-future period albeit at lower

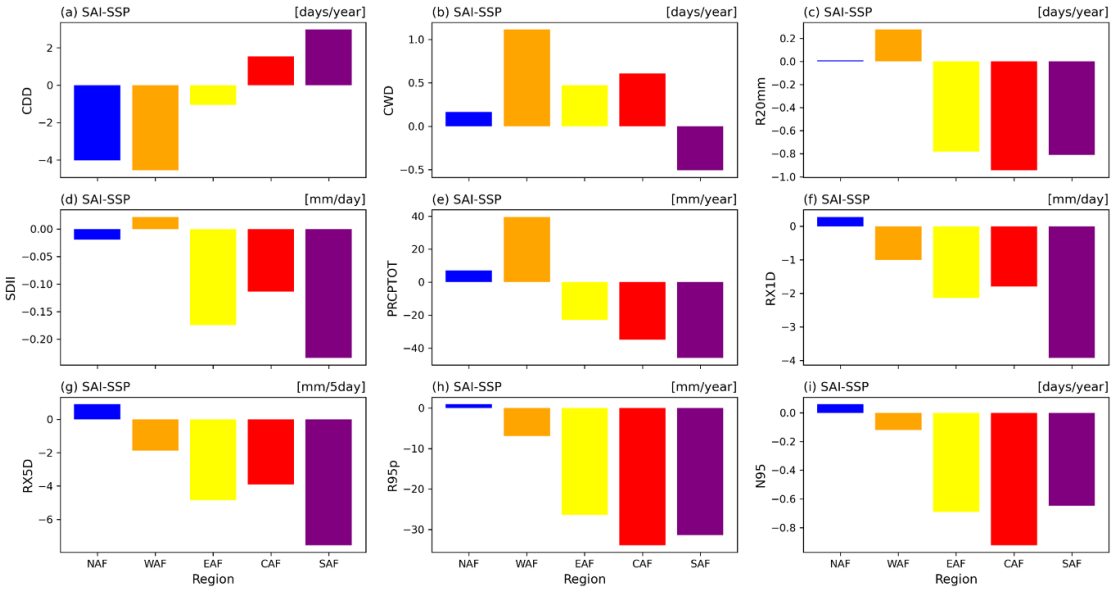

Figure 4. Projected mean regional differences between SAI and SSP2-4.5 scenario for precipitation extreme indices for the mid-future period (2050–2069). Shown are consecutive dry days (CDD; d yr^{-1}), consecutive wet days (CWD; d yr^{-1}), very heavy precipitation days (R20mm; d yr^{-1}), simple daily intensity index (SDII; mm d^{-1}), annual wet-day precipitation total (PRCPTOT; mm yr^{-1}), annual maximum 1-day precipitation (RX1D; mm d^{-1}), annual maximum 5 d precipitation (RX5D; mm 5 d^{-1}), annual precipitation from wettest days (R95p; mm yr^{-1}), and frequency of wettest days (N95; days yr^{-1}). Regions are North (NAF), West (WAF), East (EAF), Central (CAF), and Southern (SAF) Africa. Positive values indicate higher index values under SAI relative to SSP2-4.5; negative values indicate reductions.

magnitudes. It is also worth noting that different SAI strategies may yield different outcomes for these responses.

3.2.3. Quantifying changes in precipitation extreme indices

We quantify the changes in precipitation extremes by examining the mean differences between SAI and SSP2-4.5 scenario for the five African subregions (figure 4). The analysis highlights considerable regional heterogeneity in SAI impacts relative to SSP2-4.5.

For CDD, we find reductions of about 4 d yr^{-1} over NAF and WAF, whereas CAF and SAF experience notable increases (∼2–3 d yr^{-1}) suggesting SAI may enhance dryness in the southern regions while alleviating it in parts of the north and west. In contrast, CWD show modest increases in WAF and CAF (∼0.5–1 d yr^{-1}) but decrease in SAF (−0.5 d yr^{-1}) indicating potential reduction in wet spells. The R20 mm index exhibits widespread declines, with CAF and SAF showing the most pronounced reductions (approaching −1 d yr^{-1}). The SDII also consistently decreases across all regions, with strongest signal in SAF (∼−0.2 d yr^{-1}), implying lower daily rainfall intensity under SAI relative to SSP2-4.5.

For PRCPTOT is projected to increase over WAF (+30 mm yr^{-1}), but decline sharply in EAF, CAF and SAF (up to −40 mm yr^{-1}). This spatial contrast underscores the differentiated hydrological response to SAI across Africa. Extreme precipitation metrics; RX1D, RX5D, and R95p follow similar patterns, with marked reductions in SAF and CAF (up to −4 mm d^{-1} for RX1D and −6 mm 5 d^{-1} for RX5D in SAF), highlighting a substantial weakening of extreme rainfall events. Lastly, the N95 index suggests a consistent reduction in extreme wet days across CAF, SAF, and EAF (up to −0.8 d yr^{-1}), whereas changes in NAF remain minimal.

In the near-future period (figures S6 and S7), reductions in extreme wet-day indices, such as RX1D, RX5D, R95p, and N95, are evident but generally smaller in magnitude compared to the mid-future period, particularly over CAF and SAF, where mid-future declines are nearly twice as large. Similarly, decreases in SDII and PRCPTOT are more modest in the near future but intensify by mid-century, with SAF showing the most pronounced reductions. Changes in CDD and CWD exhibit consistent spatial patterns across both periods, though with stronger responses in the mid future, notably the larger increases in CDD over SAF and CAF. These results highlight that the dampening effect of SAI on extreme rainfall and wet-day totals strengthens over time, underscoring the growing hydrological divergence from SSP2-4.5 as the century progresses. These findings are consistent with previous studies (e.g. Camilloni *et al* 2022, Tye *et al* 2022), which report that SAI generally reduces the intensity and frequency of extreme rainfall, particularly in regions where SSP2-4.5 would otherwise lead to intensification.

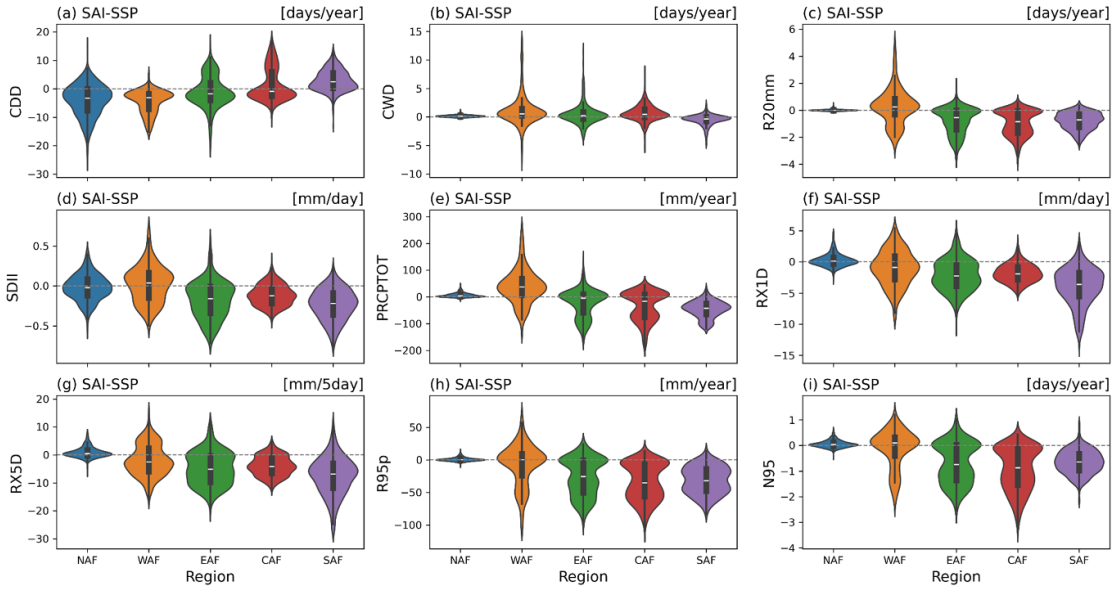

Figure 5. Violin plots showing the Kernel density estimation (KDE) for indices during the mid-future period (2050–2069). Plots show the difference in distributions calculated as SAI—SSP. The colors blue, orange, green, red, and purple represent North (NAF), West (WAF), East (EAF), Central (CAF), and Southern (SAF) Africa, respectively.

The KDE plots (figure 5) illustrate the probability distribution of the temporal average anomalies in the ensemble members relative to the mean value of the control. Longer tails represent more extreme cases, indicating a higher likelihood of occurrence. In figure 5, values on the positive side indicate increases in the index under SAI1.5 relative to SSP2-4.5, while negative values reflect the opposite. Generally, figure 5 shows longer and thinner tails for most indices and regions. For example, in figure 5(a), CDD shows a higher probability of reduction under SAI-1.5 relative to SSP2-4.5 in most regions, with a mean shift of approximately −2 d. This suggests that under SAI-1.5, CDD is projected to decrease by about 2 d in most areas, particularly pronounced over NAF, WAF, and EAF.

For CWD, the average change across most regions is ∼0 (as shown by the white dashed lines within the KDE plots), although the distributions exhibit longer tails on both sides, indicating varied responses under SAI-1.5. These results align with the spatial patterns shown in figure 3 (row 2).

The KDE plots for R20 mm and SDII suggest average decreases of ∼2 d yr^{-1} and ∼0 d yr^{-1}, respectively. Notably, PRCPTOT is generally projected to decrease by ∼25–50 mm in EAF, CAF, and SAF, while WAF emerges as the most sensitive region, with a marked increase and a more dispersed distribution.

Declines are also projected for RX1D, RX5D, R95p, and N95 in EAF, CAF, SAF, and WAF. We should mention that NAF shows smaller distributions centered around 0 for most indices, suggesting minimal changes under SAI-1.5 relative to SSP2-4.5. These findings are consistent with the smaller changes presented over NAF in earlier figures. Our results for the mid-future period (figure 5) are generally in tandem with results for the near-future period (figure S8), however, the intensities of observed changes are smaller compared to the mid-future results (see supplementary figures S8–S12).

4. Conclusion

SAI has been proposed as a potential method to offset some impacts of global warming, serving as a temporary measure while more comprehensive strategies to reduce anthropogenic carbon emissions are implemented (Keith and Irvine 2016, MacMartin *et al* 2018, Tilmes *et al* 2020). However, it is widely recognized that SAI broadly could produce both benefits and drawbacks, thus thorough evaluation of the associated trade-offs and risks (Carlson and Trisos 2018, Usha *et al* 2024) is crucial. To contribute to this ongoing discussion, we have provided an assessment of the projected changes in extreme precipitation over Africa under the SSP2-4.5 medium-range emission scenario with a focus on the mid-future (2050–2069) relative to the control period (2015–2035).

Our results show that SAI1.5 substantially alters the precipitation response over Africa. SAI1.5 counteracts much of the projected decrease in total precipitation (PRCPTOT) over WAF, confining the drying signal to its southern portion. At the same time, it reverses the large SSP2-4.5-driven increases over EAF and CAF, resulting in widespread reductions in total precipitation. These shifts suggest that SAI1.5

introduces a redistribution of hydroclimate responses rather than a uniform dampening. Notably, the reduction in PRCPTOT seen in this SSP2-4.5 medium emissions scenario agrees with findings under the high-emissions scenarios, RCP8.5 (Da-Allada *et al* 2020, Pinto *et al* 2020, Patel *et al* 2023).

SAI1.5 significantly dampens increases in extreme precipitation indices such as RX1D, RX5D, R95p, N95, and SDII, all of which are projected to intensify under SSP2-4.5. For instance, regional mean differences between SAI1.5 and SSP2-4.5 scenario show a consistent decrease across WAF, EAF, CAF and SAF for these indices. These effects are consistent across both near-and mid-future periods and align with earlier studies suggesting that SAI may suppress the frequency and intensity of very wet days by shifting rainfall distributions toward more moderate events (Camilloni *et al* 2022, Tye *et al* 2022). Such changes may reduce flood risk in some regions but could also impact water availability in areas that depend on intense rainfall events to meet seasonal water needs.

The influence of SAI1.5 on dry and wet spell behavior is similarly complex and regionally varied. CDD increase substantially in southern Africa and parts of CAF, while decreasing across NAF, WAF, and SAF. These shifts may exacerbate drought risk in already water-stressed southern regions, e.g. NAF. Conversely, CWD are projected to increase under SAI1.5 in CAF and western WAF, while decreasing over EAF and SAF, suggesting a potential reduction in flood risk in some areas but a possible increase elsewhere. The R20mm index, which reflects very heavy rainfall days, consistently declines under SAI1.5, particularly in regions where such events are projected to increase under SSP2-4.5. Similarly, the SDII index, representing mean rainfall intensity on wet days, is reduced across large parts of the continent under SAI1.5.

A test of the hydrological sensitivity shows that the sign of the change is robust when scaled using the GMST change for each scenario (see supplemental information figures S3 and S4). Although the overall precipitation signal is weaker under SAI1.5, consistent with its reduced warming, the precipitation change per degree of warming (hydrological sensitivity) is often larger in magnitude under SAI1.5 compared to SSP2-4.5. For instance, over WAF the change is larger under SAI1.5 in comparison to SSP2-4.5 per °C.

We emphasize that these findings are based on a single model (CESM2) and a single stabilization scenario (SSP2-4.5) using the ARISE-SAI-1.5 experimental design. As such, the conclusions should be interpreted within this framing. Different models, SAI deployment strategies, or emission pathways, such as SSP3-7.0 and SSP4-6.0 could yield substantially different results (e.g. Pinto *et al* 2020, Tye *et al* 2022). To enhance the robustness and credibility of future assessments, additional model intercomparison efforts are needed, and similar analyses are proposed to be applied to existing and upcoming simulations within the Geoengineering Model Intercomparison Project (Visioni *et al* 2022). Adding to this, further research is also needed to understand why these patterns occur. The aforementioned would help constrain uncertainties and better inform decision-making, especially for climate-sensitive sectors across Africa.

Data availability statement

Complete output from all 10 members of CESM2(WACCM6) SSP2-4.5 simulations and ARISE-SAI simulations is freely available on the NCAR Climate Data Gateway at http://doi.org/10.26024/0cs0-ev98 (Mills *et al* 2025) and http://doi.org/10.5065/9kcn-9y79 (Richter 2021), respectively. The ARISE-SAI and SSP2-4.5 datasets are additionally available for free download through the Amazon/AWS Open Data program. These can be accessed at https://registry.opendata.aws/ncar-cesm2-arise/ (Richter *et al* 2022). The data presented in this paper are available at http://doi.org/10.5281/ZENODO.7552583 (Tye 2023).

Acknowledgment

This material is based upon work supported by NSF National Center for Atmospheric Research (NSF NCAR), which is a major facility sponsored by the National Science Foundation (NSF) under Cooperative Agreement No. 1852977. Computing and data storage resources were provided by the Climate Simulation Laboratory at NCAR's Computational and Information Systems Laboratory (CISL). The CESM project is supported primarily by NSF. Cloud storage support is provided through the Amazon Sustainability Data Initiative.

Conflict of interest

The contact author has declared that none of the authors has any competing interests.

Author contributions

K.A.Q and M.R.T. conceptualized the study and designed the methodology. K.A.Q and K.T.Q conducted the formal analysis. K.A.Q. curated the data, while K.A.Q. and K.T.Q drafted the manuscript. S.T., I.R.S., F.N.,

T.S.E, R.C.O., and N.A.B.K. reviewed the manuscript, and M.R.T., S.T., I.R.S. supervised and managed the project.

References

Akinsanola A A, Zhou W, Zhou T and Keenlyside N 2020 Amplification of synoptic to annual variability of West African summer monsoon rainfall under global warming *npj Clim. Atmos. Sci.* **3** 21

Bingaman D C, Rice C V, Smith W and Vogel P 2020 A stratospheric aerosol injection Lofter aircraft concept: brimstone angel *AIAA Scitech 2020 Forum* p 0618

Blunden J, Boyer T, Blunden J and Boyer T (eds) 2024 State of the climate in 2023 *Bull. Am. Meteorol. Soc.* **105** Si–S483

Burns E T, Flegal J A, Keith D W, Mahajan A, Tingley D and Wagner G 2016 What do people think when they think about solar geoengineering? A review of empirical social science literature, and prospects for future research *Earth's Future* **4** 536–42

Camilloni I A, Montroull N, Gulizia C and Saurral R 2022 La Plata basin hydroclimate response to solar radiation modification with stratospheric aerosol injection *Front. Clim.* **4** 763983

Carlson C J and Trisos C H 2018 Climate engineering needs a clean bill of health *Nat. Clim. Change* **8** 843–5

Crutzen P J 2006 Albedo enhancement by stratospheric sulfur injections: a contribution to resolve a policy dilemma? *Clim. Change* **77** 211–9

Da-Allada C Y *et al* 2020 Changes in West African summer monsoon precipitation under stratospheric aerosol geoengineering *Earth's Future* **8** e2020EF001595

Danabasoglu G, Lamarque J F, Bacmeister J, Bailey D A, DuVivier A K, Edwards J and Strand W G 2020 The community earth system model version 2 (CESM2) *J. Adv. Model. Earth Syst.* **12** e2019MS001916

Di Baldassarre G, Montanari A, Lins H, Koutsoyiannis D, Brandimarte L and Blöschl G 2010 Flood fatalities in Africa: from diagnosis to mitigation *Geophys. Res. Lett.* **37** L22402

Donat M G, Sillmann J and Fischer E M 2020 Changes in climate extremes in observations and climate model simulations. From the past to the future *Climate Extremes and their implications for impact and risk assessment* 31–57

Funk C *et al* 2015 The climate hazards infrared precipitation with stations—a new environmental record for monitoring extremes *Sci Data* **2** 150066

Gbode I E, Babalola T E, Diro G T and Intsiful J D 2023 Assessment of ERA5 and ERA-interim in reproducing mean and extreme climates over West Africa *Adv. Atmos. Sci.* **40** 570–86

Gettelman A *et al* 2019 The whole atmosphere community climate model version 6 (WACCM6) *J. Geophys. Res. Atmos.* **124** 12380–403

Haile G G, Tang Q, Hosseini-Moghari S-M, Liu X, Gebremicael T G, Leng G, Kebede A, Xu X and Yun X 2020 Projected impacts of climate change on drought patterns over East Africa *Earth's Future* **8** e2020EF001502

Hausfather Z and Peters G P 2020a Emissions–the 'business as usual' story is misleading *Nature* **577** 618–20

Hawkins E, Smith R S, Gregory J M and Stainforth D A 2016 Irreducible uncertainty in near-term climate projections *Clim. Dyn.* **46** 3807–19

IPCC 2021 Climate change 2021: the physical science basis *Contribution of Working Group I to the Sixth Assessment Report of the Intergovernmental Panel on Climate Change* ed V Masson-Delmotte *et al* (Cambridge University Press) p 2391

Irvine P J and Keith D W 2020 Halving warming with stratospheric aerosol geoengineering moderates policy-relevant climate hazards *Environ. Res. Lett.* **15** 044011

Irvine P J, Kravitz B, Lawrence M G and Muri H 2016 An overview of the Earth system science of solar geoengineering *Wiley Interdiscip. Rev.* **7** 815–33

Irvine P, Emanuel K, He J, Horowitz L W, Vecchi G and Keith D 2019 Halving warming with idealized solar geoengineering moderates key climate hazards *Nat. Clim. Chang.* **9** 295–9

Ji D, Fang S, Curry C L, Kashimura H, Watanabe S, Cole J N S, Lenton A, Muri H, Kravitz B and Moore J C 2018 Extreme temperature and precipitation response to solar dimming and stratospheric aerosol geoengineering *Atmos. Chem. Phys.* **18** 10133–56

Keith D W and Irvine P J 2016 Solar geoengineering could substantially reduce climate risks—a research hypothesis for the next decade *Earth's Future* **4** 549–59

Klutse N A B *et al* 2018 Potential impact of 1.5 C and 2 C global warming on consecutive dry and wet days over West Africa *Environ. Res. Lett.* **13** 055013

Kravitz B, MacMartin D G, Mills M J, Richter J H, Tilmes S, Lamarque J F, Tribbia J J and Vitt F 2017 First simulations of designing stratospheric sulfate aerosol geoengineering to meet multiple simultaneous climate objectives *J. Geophys. Res. Atmos.* **122** 12–616

Kumi N and Abiodun B J 2018 Potential impacts of 1.5 C and 2 C global warming on rainfall onset, cessation and length of rainy season in West Africa *Environ. Res. Lett.* **13** 055009

Liu Z, Lang X and Jiang D 2022 Impact of stratospheric aerosol intervention geoengineering on surface air temperature in China: a surface energy budget perspective *Atmos. Chem. Phys. Discuss.* **2021** 1–29

Lydersen S 2014 Statistical review: frequently given comments *Ann. Rheum. Dis.* **74** 323–5

MacMartin D G, Ricke K L and Keith D W 2018 Solar geoengineering as part of an overall strategy for meeting the 1.5°C Paris target Phil. Trans. R. Soc. A. **376** 20160454

MacMartin D G, Visioni D, Kravitz B, Richter J H, Felgenhauer T, Lee W R, Morrow D R, Parson E A and Sugiyama M 2022 Scenarios for modeling solar radiation modification *Proc. Natl Acad. Sci.* **119** e2202230119

MacMartin D G, Wang W, Kravitz B, Tilmes S, Richter J H and Mills M J 2019 Timescale for detecting the climate response to stratospheric aerosol geoengineering *J. Geophys. Res. Atmos.* **124** 1233–47

Mills M J, Richter J H, Tilmes S, Kravitz B, MacMartin D G, Vitt F and Emmons L K 2017 Radiative and chemical response to interactive stratospheric sulfate aerosols in fully coupled CESM1(WACCM) *J. Geophys. Res. Atmos.* **122** 13061–78

Mills M, Visioni D and Richter J 2025 CESM2 WACCM6 SSP245 (available at: https://rda.ucar.edu/datasets/d651045/)

Niang I, Ruppel O C, Abdrabo M A, Essel C, Lennard C, Padgham J and Urquhart P 2014 Africa *Climate Change 2014: Impacts, Adaptation, and Vulnerability. Part B: Regional Aspects. Contribution of Working Group II to the Fifth Assessment Report of the Intergovernmental Panel on Climate Change* ed V R Barros *et al* (Cambridge University Press) pp 1199–265

Nikulin G, Jones C, Giorgi F, Asrar G, Büchner M, Cerezo-Mota R and Sushama L 2012 Precipitation climatology in an ensemble of CORDEX-Africa regional climate simulations *J. Clim.* **25** 6057–78

O'Neill B C, Tebaldi C, Van Vuuren D P, Eyring V, Friedlingstein P, Hurtt G and Sanderson B M 2016 The scenario model intercomparison project (ScenarioMIP) for CMIP6 *Geosci. Model Dev.* **9** 3461–82

Patel T D, Odoulami R C, Pinto I, Egbebiyi T S, Lennard C, Abiodun B J and New M 2023 Potential impact of stratospheric aerosol geoengineering on projected temperature and precipitation extremes in South Africa *Environ. Res.* **2** 035004
Pinto I, Jack C, Lennard C, Tilmes S and Odoulami R C 2020 Africa's climate response to solar radiation management with stratospheric aerosol *Geophys. Res. Lett.* **47** e2019GL086047
Quagraine K A, Nkrumah F, Klein C, Klutse N A B and Quagraine K T 2020 West African summer monsoon precipitation variability as represented by reanalysis datasets *Climate* **8** 111
Richter J H, Visioni D, MacMartin D G, Bailey D A, Rosenbloom N, Dobbins B, Lee W R, Tye M and Lamarque J-F 2022 Assessing Responses and Impacts of Solar climate intervention on the Earth system with stratospheric aerosol injection (ARISE-SAI): protocol and initial results from the first simulations *Geosci. Model Dev.* **15** 8221–43
Richter Y 2021 Assessing responses and impacts of solar climate intervention on the Earth system with stratospheric aerosol injection (ARISE-SAI) dataset (https://doi.org/10.5065/9kcn-9y79)
Robock A, Marquardt A, Kravitz B and Stenchikov G 2009 Benefits, risks, and costs of stratospheric geoengineering *Geophys. Res. Lett.* **36** L19703
Robock A, Oman L and Stenchikov G L 2008 Regional climate responses to geoengineering with tropical and Arctic SO_2 injections *J. Geophys. Res. Atmos.* **113** D16101
Serdeczny O, Adams S, Baarsch F, Coumou D, Robinson A, Hare W, Schaeffer M, Perrette M and Reinhardt J 2017 Climate change impacts in Sub-Saharan Africa: from physical changes to their social repercussions *Reg. Environ. Change* **17** 1585–600
Simanjuntak C, Gaiser T, Ahrends H E, Ceglar A, Singh M, Ewert F and Srivastava A K 2023 Impact of climate extreme events and their causality on maize yield in South Africa *Sci. Rep.* **13** 12462
Snedecor G and William G 1989 Book Review: Statistical Methods, 8th Edition George W. Snedecor and William G. Cochran Ames: Iowa State University Press, 1989. xix + 491 pp JEBS **19** 304–7
Sylla M B *et al* 2016 Climate change over West Africa: recent trends and future projections *Adaptation to climate change and variability in rural West Africa* 25–40
Sylla M B, Giorgi F, Coppola E and Mariotti L 2013 Uncertainties in daily rainfall over Africa: assessment of gridded observation products and evaluation of a regional climate model simulation *Int. J. Climatol.* **33** 1805–17
Tilmes S *et al* 2018 CESM1 (WACCM) stratospheric aerosol geoengineering large ensemble project *Bull. Am. Meteorol. Soc.* **99** 2361–71
Tilmes S *et al* 2020 Reaching 1.5 and 2.0○ C global surface temperature targets using stratospheric aerosol geoengineering *Earth Syst. Dyn.* **11** 579–601
Tye M R 2023 ARISE-SAI 1.5: CESM2 extreme temperature and precipitation indices (version 1.0.0) *Zenodo* (https://doi.org/10.5281/ZENODO.7552583)
Tye M R, Dagon K, Molina M J, Richter J H, Visioni D, Kravitz B and Tilmes S 2022 Indices of extremes: geographic patterns of change in extremes and associated vegetation impacts under climate intervention *Earth Syst. Dyn.* **13** 1233–57
Usha K H, Govindasamy B and Anu X 2024 Sensitivity of the global hydrological cycle to the altitude of stratospheric sulphate aerosol layer *Environ. Res. Lett.* **19** 084024
Visioni D, Kravitz B, Robock A, Tilmes S, Haywood J M, Boucher O and Muri H 2022 Opinion: the scientific and community-building roles of the Geoengineering Model Intercomparison Project (GeoMIP)-past, present, and future *Atmos. Chem. Phys. Discuss.* **2022** 1–44
Vogel E, Donat M G, Alexander L V, Meinshausen M, Ray D K, Karoly D, Meinshausen N and Frieler K 2019 The effects of climate extremes on global agricultural yields *Environ. Res. Lett.* **14** 054010
Zhang X, Alexander L, Hegerl G C, Jones P, Tank A K, Peterson T C and Zwiers F W 2011 Indices for monitoring changes in extremes based on daily temperature and precipitation data *Wiley Interdiscip. Rev.* **2** 851–70